RSC Advances

ROYAL SOCIETY OF CHEMISTRY

www.rsc.org/advances

A Dual Soft-Template Synthesis of Hollow Mesoporous Silica Spheres Decorated with Pt Nanoparticles as CO Oxidation Catalyst

Yunqi Li,[a,b] Bishnu Prasad Bastakoti*[a,c], Hideki Abe[a], Zongwen Liu[c], Andrew Minett[c], Zeid A. Alothman[d], and Yusuke Yamauchi*[a,b]

[a] World Premier International (WPI) Research Center for Materials Nanoarchitectonics (MANA) & Environmental Remediation Materials Unit, National Institute for Materials Science (NIMS), 1-1 Namiki, Tsukuba, Ibaraki 305-0044 (Japan)

[b] Faculty of Science and Engineering, Waseda University, 3-4-1 Okubo, Shinjuku, Tokyo 169-8555 (Japan)

[c] School of Chemical Engineering, J01, Darlington, 2006, The University of Sydney NSW, Australia

[d] Department of Chemistry, College of Science, King Saud University, Riyadh 11451, Saudi Arabia

E-mails: bishnubastakoti@hotmail.com; Yamauchi.Yusuke@nims.go.jp

Abstract

Hollow mesoporous silica (HMS) decorated with fine Pt nanoparticles are directly prepared through a dual soft-template system, using a triblock copolymer poly(styrene-*b*-2-vinyl pyridine-*b*-ethylene oxide) and a cationic surfactant cetyltrimethylammonium bromide. The Pt nanoparticles with uniform particle sizes are stably embedded inside the mesoporous silica shell having both huge surface area and large total pore volume. The Pt nanoparticles supported by the mesoporous silica exhibit excellent thermal stability, which enables the application toward high temperature CO oxidation.

1. Introduction

Fuel cells have attracted more attentions due to the depletion of fossil fuels and the serious environmental problems. The high demand of clean energy is extremely urgent, such as the polymer-electrolyte membrane fuel cell (PEMFC), which possesses absolute advantages in electric vehicle filed, however, CO poisoning of anode suppressed its development.[1] Active metal-supported catalysts (*e.g.*, Au, Pt, Pd, Rh, Ir) have been usually employed to preferential removal of CO in fuel cells.[2] The earliest discovered Pt-supported catalyst still plays a vital role until present,[3] even if the Au-supported catalysts exhibit the highest activity for CO oxidation[4] due to sensitive preparation process.[5]

The support materials also make contribution to the catalytic performance. The effect of metal-oxide interface on CO catalytic oxidation has been investigated.[6] Various oxides (*e.g.*, alumina, zeolites, silica) with porous structures and large pore volumes possess beneficial effect on the dispersion of metal nano catalysts and the easy access of metal surface.[7-9] There are two major synthesis methods. The direct deposition of metal sources (*e.g.*, K_2PtCl_4, $HAuCl_4$, H_2PdCl_4) by reducing agents[10,11] or the dispersion of metal nanoparticles by sonication[12] over inorganic substrates. Chemical vapor deposition[13] and sputtering technique[14] have also been utilized.

In order to realize excellent catalytic activity, the sufficiently exposed active sites of catalyst is necessary. Well-designed metal catalysts with proper particle sizes and shapes, and their uniform distribution are quite important factors. Due to recent advance in colloidal chemistry, organic capping agents (*e.g.*, polyvinylpyrrolidone, PVP) enable to control the morphology and distribution of metal nanoparticles in solution.[15] But, metal nanoparticles can easily deform and aggregate during or after decomposition of organic capping agents at high-temperature (> 300 ^{o}C).[16] The use of inorganic material as supports is a good solution to overcome the aforementioned problem and design excellent catalysts. Somorjai et al. recently reported thermally stable core-shell Pt/SiO_2 nanocatalysts. The mesoporous SiO_2 shell plays a crucial role to isolate Pt nanoparticles and provide synergistic effect in high temperature CO oxidation reaction.[17]

In this paper, we have strongly anchored uniformly-sized Pt nanoparticles inside the shell of hollow mesoporous silica (HMS) spheres. Our approach is based on a dual soft-template method using a core-shell-corona type triblock copolymer poly(styrene-*b*-2-vinyl pyridine-*b*-ethylene oxide) (PS-*b*-P2VP-*b*-PEO) and a cationic surfactant cetyltrimethylammonium bromide (CTAB). The hydrophobic PS frozen core in aqueous solution forms the hollow interior[18] and the surfactant CTAB directs the mesoporous structure.[19] The obtained HMS decorated with Pt nanoparticles (HMS/Pt) shows high surface area and large pore volume. The Pt nanoparticles are stably immobilized inside the mesoporous shell with the retention of the inherent metal characters. Thermally stable HMS/Pt catalyst shows excellent CO oxidation activity at high temperature.

2. Experimental

2.1 Materials

Triblock copolymer poly(styrene-*b*-2-vinyl pyridine-*b*-ethylene oxide) PS(14,500)-*b*-P2VP(20,000)-*b*-PEO(33,000) (the number in parentheses is the molecular weight of each block) with a polydispersity index 1.15 was purchased from Polymer Source. K_2PtCl_4 (Wako), polyvinyl pyrrolidone (PVP, Nacalai) (K-30, M_w 40,000), cetyltrimethylammonium bromide (CTAB, Wako), tetraethyl orthosilicate (TEOS, Wako), ethanol (Wako), 28% ammonium hydroxide ($NH_3 \cdot H_2O$, Sigma), and tetrahydrofuran (THF, Nacalai) were used without further purification.

2.2 Synthesis of HMS/Pt spheres

Two types of solution were prepared separately. 20 mg of triblock copolymer PS-*b*-P2VP-*b*-PEO was dissolved completely in 4 mL of THF. Another solution was composed of 40 mg of CTAB and 5 mg or 10 mg of PVP-capped Pt nanoparticles in 16 mL of water with 600 μL of 28% ammonia solution. The two solutions were mixed and stirred for 30 min at room temperature and added 16 mL of ethanol. After 30 min, 128 μL of TEOS in 600 μL of ethanol was added drop wise and stirred for 24 h at room temperature. The black colloidal particles were collected from centrifugation with 3 cycles of washing, dried at room temperature, and calcined at 550 ^oC for 4 h in air or N_2

environment. The obtained samples were abbreviated as HMS/Pt_*x*_*y* where *x* is the applied calcination environment [A (air) or N (nitrogen)] and *y* is the amount of Pt nanoparticles [5 (5 mg) or 10 (10 mg)]. For the preparation of PVP-capped Pt nanoparticles, 250 μL of K_2PtCl_4 solution (20 mM) and 5.5 mg of PVP were dissolved well in 9 mL of ethanol. This mixture was sealed in an autoclave and heated under 110 ^oC for 3 h.[20]

2.3 Characterization

Field emission scanning electron microscope (SEM, HITACHI SU-8000) at 2 kV and transmission electron microscope (TEM, JEOL JEM-1210) at 200 kV were operated to observe the morphology and mesostructure of the obtained HMS/Pt spheres. Belsorp 28 apparatus (Bel Japan, Inc.) was used to measure nitrogen adsorption-desorption isotherms. Brunauer-Emmett-Teller (BET) and Barrett-Joyner-Halenda (BJH) methods were used to evaluate the surface area, total pore volume, and pore size distribution. To confirm the Pt crystal structure, X-ray diffraction machine (XRD, Rigaku) with a Cu Kα radiation (40 kV, 30 mA) was used at a scanning rate of $0.5°\cdot min^{-1}$. Small-angle X-ray scattering (SAXS, Rigaku) with a Cu Kα radiation (40 kV, 30 mA) was used to measure the pore-to-pore distance. X-ray photoelectronic spectroscope (XPS) with PHI Quantera SXM (ULVAC-PHI) source was operated to determine the electronic states of Pt. Inductively coupled plasma atomic emission spectroscope (ICP-AES, SII Nano Technology Inc.) was used to determine the exact loading amount of Pt nanoparticles. Thermal gravimetric analysis (TGA) was performed by using TG-DTA machine (Hitachi HT-Seiko Instrument Exter 6300).

2.4 Catalytic CO Oxidation

Catalytic CO oxidation over the hollow mesoporous SiO_2 supported Pt nanoparticles was equipped with a gas chromatograph (Shimadzu GC-8A) using a batch reactor. 50 mL volume capacity reactor was filled with mixture gas consisting of CO and O_2 at a molar ratio of 2:1 (10 kPa). 10 mg of catalyst was placed in the circulation line of the reactor (**Scheme S1**). The gas mixture was circulated at a constant rate. The temperature was controlled with an electric tubular furnace that was surrounded by the circulation line at the catalyst position. The composition of the gas mixture

was monitored with the gas chromatograph at fixed time interval.

3. Results and Discussion

The HMS/Pt spheres were prepared by a dual soft-template system, as shown in **Figure 1**. An aqueous solution containing of PVP-capped Pt nanoparticles and CTAB were firstly prepared. The pH of the solution was adjusted to 10.5 using ammonia solution. The triblock copolymer (PS-*b*-P2VP-*b*-PEO) was dissolved as unimers in THF separately. After mixing the above two solutions, the micellization of PS-*b*-P2VP-*b*-PEO was stimulated and the spherical micelles were formed with defined core-shell-corona structure in which hydrophobic PS core is enclosed by hydrophilic P2VP shell and PEO corona. The mechanism of this dual soft-template system has been clearly investigated in our previous work.[21] PS-*b*-P2VP-*b*-PEO polymeric micelles direct the formation of the hollow interior, while CTAB surfactant works as a pore-directing agent for the mesoporous shells. Negatively charged hydrolyzed silica species enable to set up the bonding between P2VP blocks of the polymeric micelles and CTA^+ ions.

Spherical HMS/Pt nanoparticles were clearly seen under SEM in **Figure 2** and **Figure S1**, regardless of the loading amount of Pt nanoparticles (5 or 10 mg) and calcination environment (air or nitrogen). The average diameter of silica spheres is *ca.* 85 nm. The inner structure and the distribution of Pt nanoparticles were confirmed by TEM observation (**Figure 3a**). Mesoporous shell containing Pt nanoparticles surrounds a hollow center of *ca*. 17 nm. From high-resolution TEM (HRTEM) image, the lattice fringe with a *d*-spacing of 0.23 nm which is characteristic of the (111) plane clearly confirms Pt *fcc* nanocrystals (**Figure 3a**). The hollow interior can be finely tuned by changing the molecular weight of PS blocks.[22] As shown in TEM image (**Figure S2**), the diameter of PS core highlighted by 0.1 wt% phosphotungstic acid[23,24] is measured to be *ca.* 20 nm which coincides with the hollow size of HMS (*ca.* 17 nm).[21]

Nitrogen adsorption-desorption isotherms are typical type IV (**Figure 4a**). From the BJH calculation method, the average pore sizes are 2.3 nm and 2.0 nm for HMS/Pt_5_A and

HMS/Pt_5_N, respectively (**Figure 4b**). Several groups have reported the mesoporous SiO_2 materials by using CTAB, in which the obtained mesopore sizes are almost the same as our HMS/Pt spheres (**Table S1)**. In low-angle XRD profile (**Figure 4c**), a broad peak at 2.5° indicates a pore-to-pore distance of *ca.* 3.5 nm. Considering the pore sizes obtained by the BJH method, the wall thicknesses are thought to be quite thin (1.0-1.5 nm). The surface area and the pore volume are summarized in **Table S1**. The decrease of surface area is observed with the increase of loading amount of Pt nanoparticles, because Pt is a heavy element. However, compared with pure HMS without Pt nanoparticles, the decrease in surface area of HMS/Pt spheres is not so serious. It can be concluded that, even after decorated by Pt nanoparticles, the mesoporous SiO_2 shell still maintains high surface area, which provides the direct flow access of guest species (*e.g.*, CO gas) to the active metal sites.

The exact loading amount of Pt was confirmed by ICP analysis, as shown in **Table S1**. In wide-angle XRD profile (**Figure S3a**), the diffraction peaks are assigned to be (111), (200), (220) and (222) planes of Pt *fcc* crystal. The sharpness of the diffraction peaks can predict the average Pt crystal size in HMS/Pt spheres. The crystal size of Pt nanoparticles in HMS/Pt_5_A (treated in air) was found to be larger than that in HMS/Pt_5_N (treated in nitrogen). To further investigate the effect of calcination environment, the size distribution of Pt nanoparticles were evaluated by counting 100 Pt nanoparticles in TEM images (**Figure 3b**). It was found that the most frequent size of Pt in HMS/Pt_5_A (6-7 nm) is double than that in HMS/Pt_5_N (3-4 nm). XPS analysis was carried out to check the electronic states of Pt nanoparticles before catalytic CO oxidation (**Figure S3b**). Comparing with previous literatures (**Table S2**), the binding energy for double peaks of Pt $4f_{7/2}$ and Pt $4f_{5/2}$ are typical for the zero-valent Pt.

Temperature-dependent weight loss for as-prepared samples was measured by TG analysis (**Figure S4**). Under nitrogen condition, the required temperature (600 °C) to remove the templates observed by TG curve is higher than the applied temperature (550 °C) used in the experiment. However, the obtained HMS/Pt spheres have no carbon contents, because the calcination at 550 °C

was applied for 4 hours. When the calcination time is less, some carbon derivatives are still remained. As shown in TG analysis (**Figure S4**), there is a large difference of temperature-dependent weight loss between air and nitrogen conditions. When the samples are treated in nitrogen, the decomposition of organic templates delays. It means that some polymer derivatives (*e.g.*, carbon) is probably formed at the early stage of the calcination process. Therefore, thermal aggregation of the Pt nanoparticles is effectively suppressed owing to such polymer derivatives. In contrast, in the case of air condition, the organic templates are directly burned out without formation of polymer derivatives, in which the Pt nanoparticles can freely diffused, thereby occurring the nanoparticle aggregation and recrystallization.

The catalytic CO oxidation of HMS/Pt spheres was studied in a gas-circulation reactor equipment with a gas chromatograph (**Scheme S1**).[25] Under CO-dominated condition (CO and O_2 with a molar ratio of 2:1), at relative low temperature Pt surface is predominantly covered by CO, which prohibit O_2 adsorption. With the increase of applied temperature, the desorption of CO is occurred and it replaces with O_2 on the Pt surface, which is a critical step for rate determination of CO oxidation.[26,27] For both HMS/Pt_5_A and HMS/Pt_5_N, the CO conversion rate is improved with elevated temperature from 125 ^{o}C to 250 ^{o}C, as shown in **Figure 5**. In general, the size and shape of Pt nanoparticles are controllable under featured temperature and time,[28] which are critical factors to determine the performance of catalytic CO oxidation. HMS/Pt_5_A exhibits superior catalytic activity at each applied temperatures, even the loading amount of Pt is only 1.0 wt% (**Figure 5**). A full conversion of CO to CO_2 is observed at 250 ^{o}C for HMS/Pt_5_A, a quite high performance than that on HMS/Pt_5_N. The similar results have been reported so far.[29] Large-sized Pt nanoparticles have a lower activation energy for CO desorption in comparison with small-sized Pt nanoparticles.[30,31] Thus, such CO adsorbed on plane Pt surface is more reactive than on low coordination sites (*i.e.* corners and edges) for catalytic CO reaction.[32] Large-sized Pt nanoparticles calcined in air have higher proportion of Pt atoms on flat surface. Actually, several deposited Pt nanoparticles show cube- and/or octahedral-like shapes (**Figure 3a**) which have been often seen as

typical ones enclosed by low-index planes.[33] Pt nanoparticles in mesoporous silica shells of HMS/Pt spheres calcined at 550 ^{o}C are able to avoid serious thermal agglomeration and the loss of active sites at high temperature. We expect that our HMS/Pt spheres will exhibit improved CO oxidation activity if the applied temperature is increased.

4. Conclusion

We established a dual soft-template system using triblock copolymer (PS-*b*-P2VP-*b*-PEO) and cationic surfactant (CTAB) to synthesize HMS/Pt spheres. The thermally stable mesoporous SiO_2 shells possess great potential to retard the thermal agglomeration of Pt nanoparticles at high temperature and also make synergetic contribution to the catalytic activity. The obtained HMS/Pt spheres exhibit superior CO oxidation reaction activity. Our dual soft-template method highlights the significance of HMS spheres decorated with metal nanoparticles. By further tuning metal composition, shape and size of nanoparticles; we can expect huge potential applications in future.

Acknowledgement

We extend our sincere appreciation to the Deanship of Scientific Research at King Saud University for its funding this Prolific Research Group (PRG-1436-04).

References

[1] A. Chen, P. Holt-Hindle, *Chem. Rev.*, 2010, **110**, 3767-3804.

[2] K. Liu, A. Wang, T. Zhang, *ACS Catal.*, 2012, **2**, 1165-1178.

[3] J. D. Kistler, N. Chotigkrai, P. Xu, B. Enderle, P. Praserthdam, C.-Y. Chen, N. D. Browning, B. C. Gates, *Angew. Chem. Int. Ed.*, 2014, **53**, 8904-8907; *Angew. Chem.,* 2014, **126**, 9050-9053.

[4] Y. Denkwitz, B. Schumacher, G. Kučerová, R. J. Behm, *J. Catal.*, 2009, **267**, 78-88.

[5] G. R. Bamwenda, S. Tsubota, T. Nakamura, M. Haruta, *Catal. Lett.*, 1997, **44**, 83-87.

[6] K. An, S. Alayoglu, N. Musselwhite, S. Plamthottam, G. Melaet, A. E. Lindeman, G. A. Somorjai, *J. Am. Chem. Soc.*, 2013, **135**, 16689-16696.

[7] S. Zheng, L. Gao, *Mater. Chem. Phys.*, 2002, **78**, 512-517.

[8] M. M. Schubert, S. Hackenberg, A. C. van Veen, M. Muhler, V. Plzak, R. J. Behm, *J. Catal.*, 2001, **197**, 113-122.

[9] J. Singh, J. A. van Bokhoven, *Catal. Today*, 2010, **155**, 199-205.

[10] A. Fukuoka, J. Kimura, T. Oshio, Y. Sakamoto, M. Ichikawa, *J. Am. Chem. Soc.*, 2007, **129**, 10120-10125.

[11] H. Wang, H. Y. Jeong, M. Imura, L. Wang, L. Radhakrishnan, N. Fujita, T. Castle, O. Terasaki, Y. Yamauchi, *J. Am. Chem. Soc.*, 2011, **133**, 14526-14529.

[12] R. M. Rioux, H. Song, J. D. Hoefelmeyer, P. Yang, G. A. Somorjai, *J. Phys. Chem. B*, 2005, **109**, 2192-2202.

[13] M. Okumura, S. Nakamura, S. Tsubota, T. Nakamura, M. Azuma, M. Haruta, *Catal. Lett.*, 1998, **51**, 53-58.

[14] L. Armelao, D. Barreca, G. Bottaro, A. Gasparotto, E. Tondello, M. Ferroni, S. Polizzi, *Chem. Mater.*, 2004, **16**, 3331-3338.

[15] I. Pastoriza-Santos, L. M. Liz-Marzán, *Langmuir*, 2002, **18**, 2888-2894.

[16] B. P. Bastakoti, Y. Li, N. Miyamoto, N. M. Sanchez-Ballester, H. Abe, J. Ye, P. Srinivasu, Y. Yamauchi, *Chem. Commun.*, 2014, **50**, 9101-9104.

[17] S. H. Joo, J. Y. Park, C.-K. Tsung, Y. Yamada, P. Yang, G. A. Somorjai, *Nat. Mater.*, 2009, **8**, 126-131.

[18] B. P. Bastakoti, Y. Li, T. Kimura, Y. Yamauchi, *Small*, 2015, **11**, 1992-2002.

[19] J. Yang, D. Shen, L. Zhou, W. Li, X. Li, C. Yao, R. Wang, A. M. El-Toni, F. Zhang, D. Zhao, *Chem. Mater.*, 2013, **25**, 3030-3037.

[20] K.-J. Lin, L.-J. Chen, M. R. Prasad, C.-Y. Cheng, *Adv. Mater.*, 2004, **16**, 1845-1849.

[21] Y. Li, B. P. Bastakoti, M. Imura, J. Tang, A. Aldalbahi, N. L. Torad, Y. Yamauchi, *Chem. Eur. J.*, 2015, **21**, 6375-6380.

[22] B. P. Bastakoti, S. Ishihara, S.-Y. Leo, K. Ariga, K. C.-W. Wu, Y. Yamauchi, *Langmuir*, 2014, **30**, 651-659.

[23] M. Sasidharan, D. Liu, N. Gunawardhana, M. Yoshio, K. Nakashima, *J. Mater. Chem.*, 2011, **21**, 13881-13888.

[24] L. Lei, J.-F. Gohy, N. Willet, J.-X. Zhang, S. Varshney, R. Jérôme, *Polymer*, 2006, **47**, 2723-2727.

[25] G. Saravanan, H. Abe, Y. Xu, N. Sekido, H. Hirata, S. Matsumoto, H. Yoshikawa, Y. Yamabe-Mitarai, *Langmuir*, 2010, **26**, 11446-11451.

[26] S. M. McClure, M. Lundwall, Z. Zhou, F. Yang, D. W. Goodman, *Catal. Lett.,* 2009, **133**, 298-306.

[27] A. D. Allian, K. Takanabe, K. L. Fujdala, X. Hao, T. J. Truex, J. Cai, C. Buda, M. Neurock, E. Iglesia, *J. Am. Chem. Soc.*, 2011, **133**, 4498-4517.

[28] B. P. Farrell, I. V. Sevonkaev, D. V. Goia, *Platinum Met. Rev.*, 2013, **57**, 161-168.

[29] D. Varade, H. Abe, Y. Yamauchi, K. Haraguchi, *ACS Appl. Mater. Interfaces*, 2013, **5**, 11613-11617.

[30] B. Atalik, D. Uner, *J. Catal.*, 2006, **241**, 268-275.

[31] G. S. Zafiris, R. J. Gorte, *J. Catal.*, 1993, **140**, 418-423.

[32] F. J. Gracia, L. Bollmann, E. E. Wolf, J. T. Miller, A. J. Kropf, *J. Catal.*, 2003, **220**, 382-391.

[33] N. Tian, Z.-Y. Zhou, S.-G. Sun, Y. Ding, Z. L. Wang, *Science*, 2007, **316**, 732-735.

Figure 1

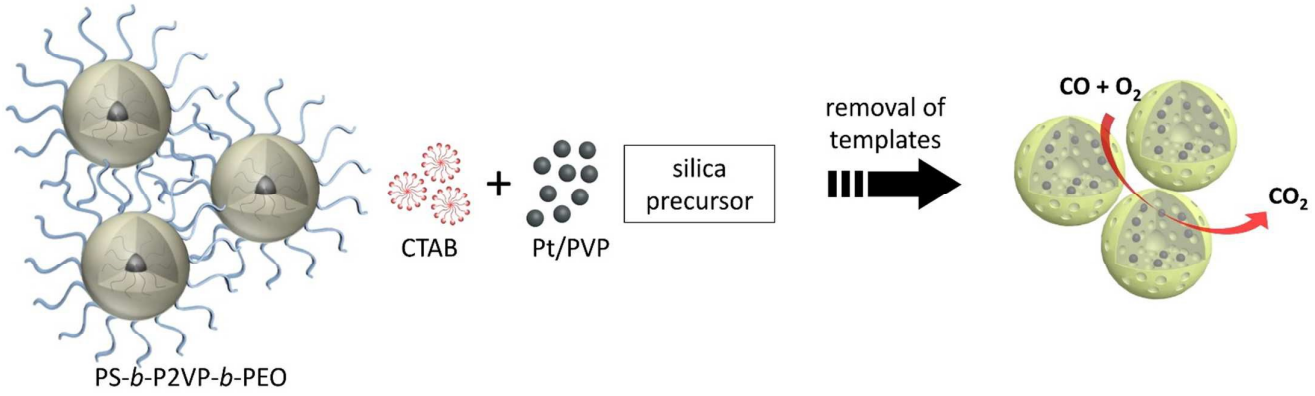

Figure 1. Schematic illustration of a dual soft-template synthesis for HMS/Pt.

Figure 2

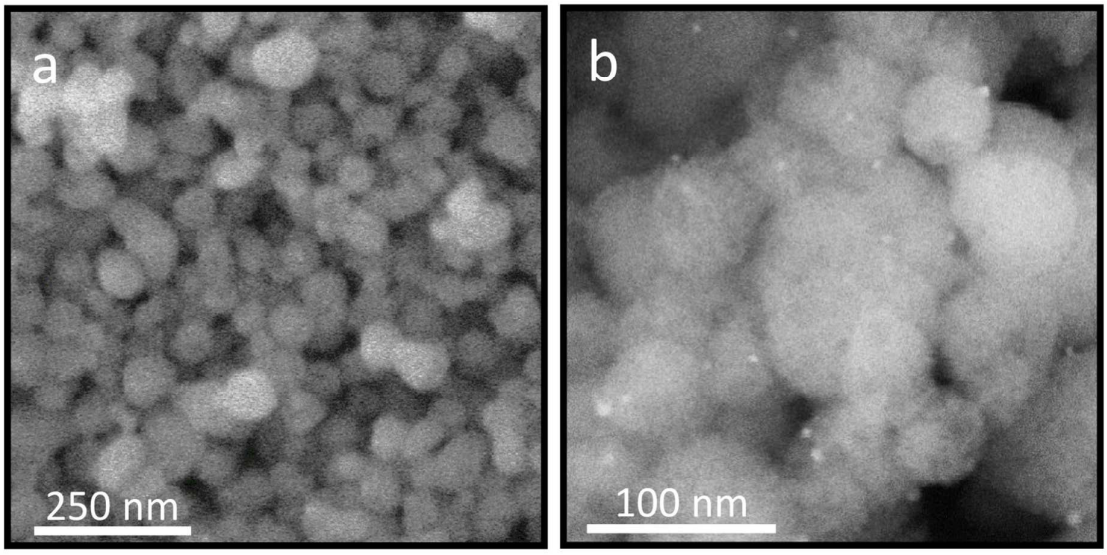

Figure 2. Low and high magnification SEM images of HMS/Pt_5_A.

Figure 3

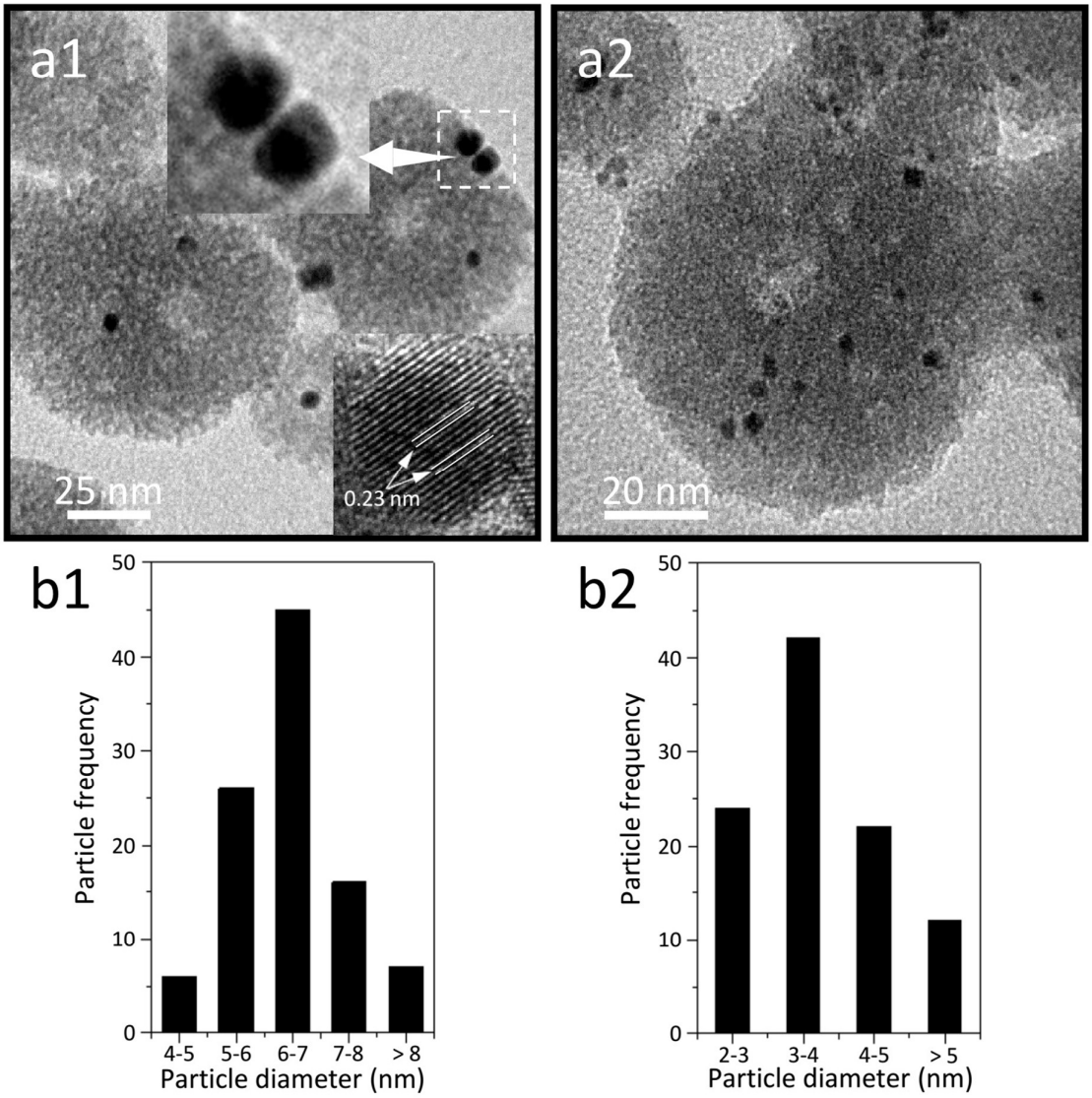

Figure 3. (a) TEM images and (b) Pt nanoparticle size distributions of (1) HMS/Pt_5_A and (b) HMS/Pt_5_N. High resolution TEM image is shown in inset.

Figure 4

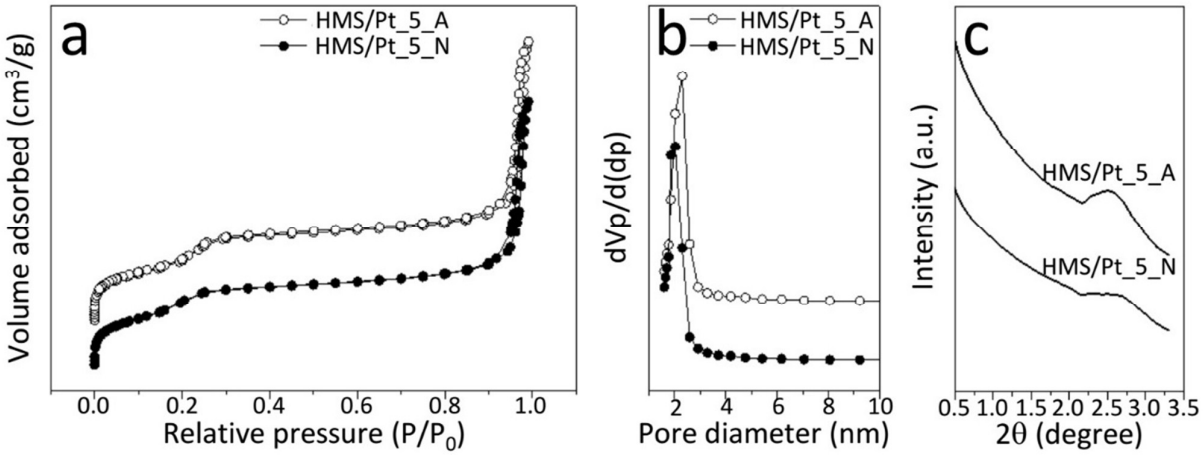

Figure 4. (a) Nitrogen adsorption-desorption isotherms, (b) pore size distribution, and (c) low-angle XRD patterns of HMS/Pt_5_A and HMS/Pt_5_N.

Figure 5

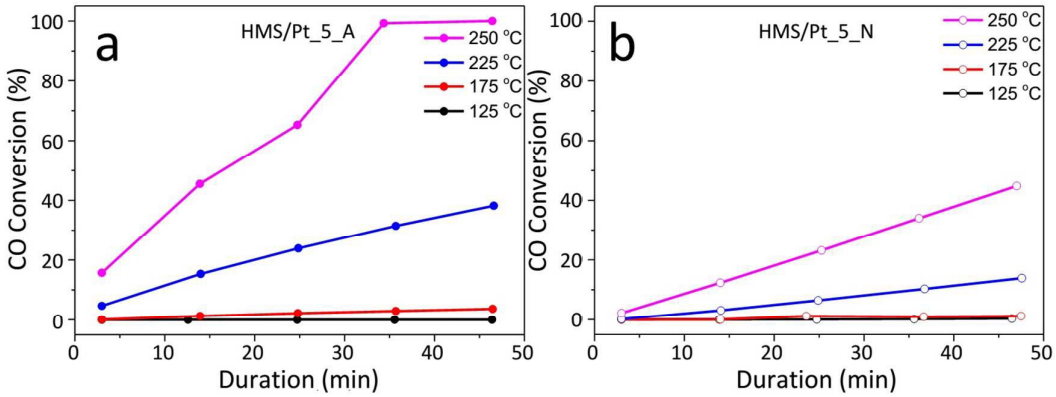

Figure 5. CO oxidation activity of (a) HMS/Pt_5_A and (b) HMS/Pt_5_N in different temperatures.

Graphical Abstract

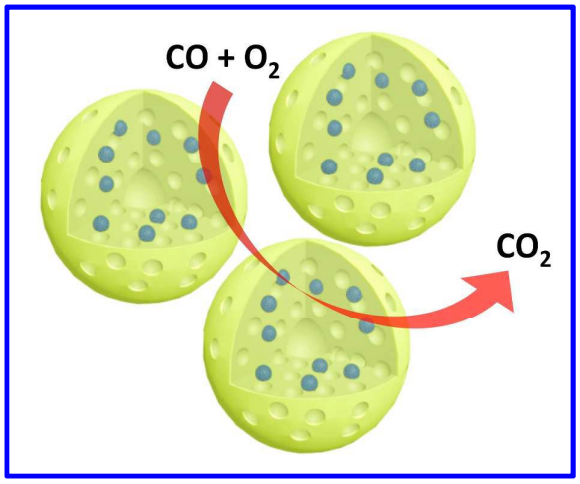

Hollow mesoporous silica spheres decorated with fine Pt nanoparticles are prepared through a dual soft-template system and used as catalyst for high temperature CO oxidation.